35th Annual International Conference of the IEEE EMBS
Osaka, Japan, 3 - 7 July, 2013

Visualization of Pulsatile CSF Motion Separated by Membrane-like Structure based on Four-dimensional Phase-contrast (4D-PC) Velocity Mapping

Satoshi Yatsushiro[1] , Akihiro Hirayama[2] , Mitsunori Matsumae[2] , Non-member, Kagayaki Kuroda[1] , *Member, IEEE*

[1] Course of Information Science and Engineering, Graduate School of Engineering, Tokai University, 4-1-1 Kitakaname, Hiratsuka, Kanagawa 259-1292, Japan

[2] Department of Neurosurgery, Tokai University School of Medicine, 143 Shimokasuya, Isehara, Kanagawa 259-1193, Japan

***Abstract*—This work was performed to indicate the usefulness of magnetic resonance (MR) 4-dimentional phase contrast (4D-PC) technique in assessing CerebroSpinal Fluid (CSF) motion in comparison with the time-Spatial Labeling Inversion Pulse (Time-SLIP) technique. 4D-velocity vector, their curl, and, pressure gradient were evaluated in both flow phantom, and normal volunteers and a patient with hydrocepharus. The velocity and pressure gradient fields obtained by the 4D-PC technique were useful to visualize the CSF dynamics under the presence of a membrane-like structure, unlike the Time-SLIP in which the spin travel was visualized. Quantitative property was another advantage of the 4D-PC. The curl and the pressure gradient fields obtained with actual units should help clinicians to classify the conditions of the patients with CSF disorders.**

I. Introduction

Principal driving forces of pulsatile CSF has not been understood completely [1]. Pressure transmission from the blood vessels and/or brain parenchyma can be regarded as driving forces for the intracranial and spinal CSF. Cardiac gated 2D-PC MR has been used to evaluate the regional CSF pulsatile motion in an attempt to understand normal CSF dynamics and to diagnose disorders such as hydrocephalus [2-3]. On the other hand, Yamada et al. have reported that travel of CSF can be visualized by means of a spin labeling technique called Time-SLIP [4]. However, comprehensive understanding of CSF movement still remains difficult. We have been developing a method to visualize spatiotemporal velocity distribution of intracranial pulsatile CSF motion by 4D-PC technique to clarify the CSF dynamics. In this study, 4D-PC experiments and image analysis have been performed with a pulsatile flow phantom to indicate the difference and the usefulness of 4D-PC technique in assessing CSF motion in comparison with the Time-SLIP especially when a membrane exists in the flow field. Then, 4D-velocity vector fields, their curl, and, pressure gradient fields were evaluated and assessed to examine whether those flow factors characterize the CSF dynamics in patients with asymptomatic arachnoid cyst with hydrocephalus.

II. Material and Method

A. Theory

In general, a vector field is fully characterized by divergence and curl of the vector field based on the Helmholtz's theorem [5]. In the CSF motion analysis here, the divergence of the flow field was ignored because no significant "welling up" motion should be observed unless extremely low velocity encoding factor is used to observe CSF generation in the choroid plexus in the ventricle. The destribution of curl [$(m^2 \cdot s)^{-1}$] was thus calculated as equation (1) to show the presence of the vortex in the velocity field.

$$curl\ \boldsymbol{v} = \nabla \times \boldsymbol{v} \qquad (1),$$

where $\boldsymbol{v}$ is a velocity vector. As is known from (1), a curl is a vector, whose direction and length respectively denote the axis and intensity of the vortex. Pressure gradient were obtained based on the Navier-Stokes equation [6] further analyze the mechanism of the flow dynamics.

$$\nabla p = -\rho\left(\frac{\partial \boldsymbol{v}}{\partial t} + \boldsymbol{v} \cdot \nabla \boldsymbol{v}\right) + \mu \cdot \nabla^2 \boldsymbol{v} \qquad (2),$$

where p is pressure, t is time, ρ is fluid density and μ is dynamic viscosity. The first term in the right hand side of (2) denotes the acceleration, while the second and third terms are the convection and viscosity, respectively. The unit of the pressure gradient was [Pa/m].

B. Phantom Experiments

Phantom experiments were performed to examine the characteristic of pulsatile flow obtained by 4D-PC and time-SLIP techniques. The phantom comprises horizontally placed acryl tubes with a diameter of 2cm as shown in Figure 1 to mimick the CSF flow in a simplified manner. The inflow was derived into two acryl tubes through a Y-shaped branch; one was equipped in its middle with a thin rubber membrane mimicking the membrane-like structure such as a thin wall of arachnoid cyst. The other was equipped with no membrane so as to allow a side flow coming from the membrane-equipped tube. The phantom was connected to a roller pump (HAD 101; Mera, Tokyo, Japan) by expansion-free flexible tubes and

plastic tubes. The physiological saline water was used to simulate CSF. The fluid was moved in a pulsatile manner by the periodic pressure of the roller pump. An artificial, 1-Hz ECG signal made by a waveform generator (HP 33120a, Agilent Technologies, Santa Clara, CA) synchronized the roller pump. The same signal synchronized the signal acquisition with a 1.5-T scanner (Gyroscan, Philips; Best, The Netherlands) via ECG cables. The mean velocity in the tube was estimated base on the flow rate [L/min] of the roller pump and the cross sectional area of the acryl tube ($1\times1\times\pi$ [cm^2]). The value was 5.3 [cm/sec] in the outflow tube at a flow rate setting of 1.00 [L/min]. The 4D-PC images were obtained with the following conditions; flow encode directions, IS, RL and AP; TR, 8.1 ms; TE, 5.6 ms; Flip angle (FA), 20°; Field of view (FOV), 30 × 30 cm^2; Velocity encoding (VENC), 10 cm/s; slice direction, coronal; and spatial resolution, 1.96 mm (isotropic). Images were acquired at 32 temporal points per a cardiac cycle and were retrospectively reconstructed.

After obtaining the velocity information in three directions, the in-plane velocities were delineated by vectors, while the through-plane velocities were visualized by colors with a custom-made software programmed with Matlab (R2010a or later, Mathworks, Natick, MA, USA). The vector-color coded CSF velocity field was then superimposed on the T_2 weighted images. Time-SLIP image were taken immediately before the 4D-PC image acquisitions with the following conditions: TR, 6,000 ms; TE, 73.8-78.7 ms, FA, 90°; slice thickness, 5 mm; FOV, 26 × 26 cm^2; acquisition matrix, 256 × 256; and inversion time (TI), 1,700-5,900 ms. Labeling was given in a region at the upper stream side in the in-flow tubes of the phantom as shown in Figure 1 to verify that no spin travels beyond the point of the membrane.

C. Volunteer Experiments

The volunteer studies were approved by the institutional review board (IRB). Appropriate informed consent was obtained for each volunteer. Image acquisitions were performed in a 22-years-old male with asymptomatic arachnoid cyst and a 22-years-old female with hydrocephalus. Most of the imaging conditions and the analysis processes were similar to the phantom experiments except for the below-mentioned.

The imaging slab was at sagittal or coronal, and the image reconstruction was synchronized retrospectively by the pulse from a finger plethysmograph. Labeling in the Time-SLIP acquisition was given in a region covering the mid portion within the arachnoid cyst. The velocity, curl and pressure gradient fields were analyzed in a quantitative manner in the aqueduct. In this anatomical location, the CSF movement can be regarded as laminar flow since the Reynolds number, R, can be estimated as $R \approx 136 << 2000$. The velocity and pressure gradient in the aqueduct was obtained along the maximum velocity line in the oblique saggital plane as shown in the schematic diagram in Figure 2. In this particular analysis the RL flow was ignored for simplicity. The velocity vectors along the duct was then classified as positive when $v_{FH} > 0 \cup v_{AP} < 0$. while as negative when $v_{FH} < 0 \cup v_{AP} > 0$.

For comparison of the quantitative flow a number of healthy volunteers, 19 male and 19 female with mean age of 50, were also performed.

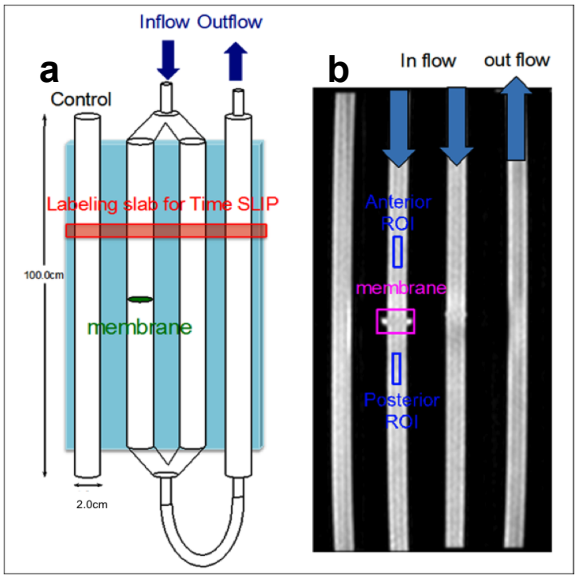

Figure 1. The pulsatile phantom shown with the imaging slab common for the two different imaging techniques and the excitation slab for the Time-SLIP (a), and a T2 weighted coronal view (b)

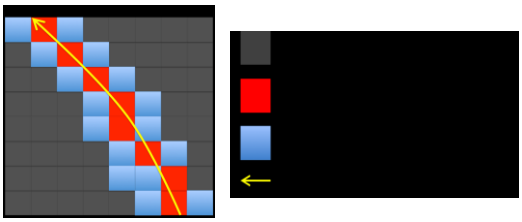

Figure 2. Schematic diagram of the maximum velocity line for quantitative analysis of the velocity and pressure gradient.

III. Result

Results of the phantom measurements are shown in Figure 3. In the Time-SLIP image in (b), the labeled fluid exhibited patterns of laminar flows with a maximum displacement at the center of the inflow tube without membrane, while in the tube with membrane, the labeled fluid showed small displacement of approximately 1 [cm] and thus, no spin traveling was observed beyond the position of the membrane. The 4D-PC velocity image in (a) presented similar flow pattern in the tube without membrane. In contrast to the Time-SLIP result, an oscillating fluid propagation beyond the membrane was observed in the tube with the membrane. Temporal changes of the mean velocity within the region-of-interest (ROI) in the upper and lower stream positions of the membrane (the blue squares in Figure 1(b)) are compared in Figure 4. The waveform in the upper- stream ROI exhibited similarity with that in the lower-stream ROI with a slightly lowered peak-to-peak amplitude.

In the morphological image of the patient with the arachnoid cyst, the cyst located around the falx cerebelli was clearly recognized as shown in Figure 5 (a) (blue arrows). Zoomed 4D-PC velocity map in the region including the infratentorial (red square in (a)) are shown in (c) and (d) at

9.3% and 81.3% of time periods in a peripheral pulse cycle. The corresponding Time-SLIP image with labeling slab in the mid of the arachnoid cyst (orange rectangle) is shown in (b). In the 4D-PC images, a relatively small but clear oscillating motion was observed within the arachnoid cyst (red arrow head). In contrast, no displacement of the labeled CSF in this anatomical location was seen in the Time-SLIP image.

Temporal changes of the 4D-PC velocity, curl and pressure gradient images in the ventricular system of the patient with hydrocephalus are shown in Figure 6, 7 and 8, respectively. The images exhibited enlarged lateral and third ventricles due to obstruction at the aqueduct. The 4D-PC velocity image in the aqueduct in Figure 6 showed slightly lowered velocity amplitude because of the membrane in the aqueduct (red circle). However, propagation of the pulsatile CSF motion and/or pressure through the membrane within the aqueduct was not clear. Thus the quantitative analysis was necessary.

The results are shown in Figure. 9 (a), (b) and (c). The peak-to-peak flow amplitude in the patient was obviously lower than that in the mean in the healthy volunteer group. The other indicators like curl and pressure gradient were also lower than those in the healthy volunteers.

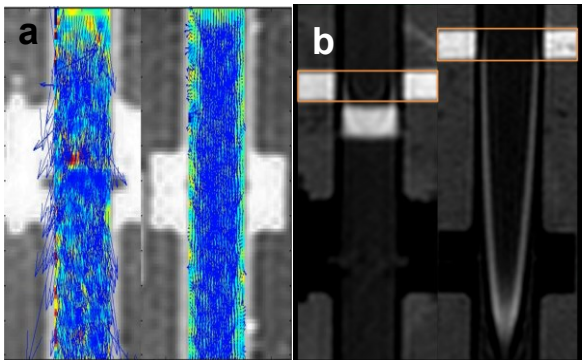

Figure 3. Flows in the phantom visualized by 4D-PC (a) and Time-SLIP (b). In each image, the tube on the left hand side was with the membrane.

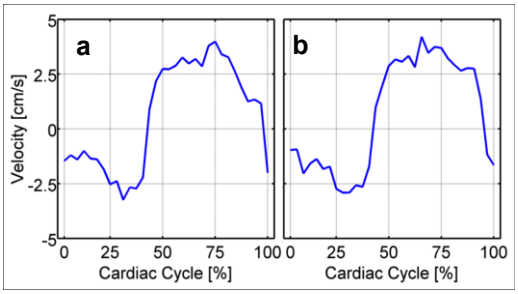

Figure 4. Temporal changes of the mean velocity in the upper stream (a) and in the lower stream ROI's around the membrane shown in Figure 1.

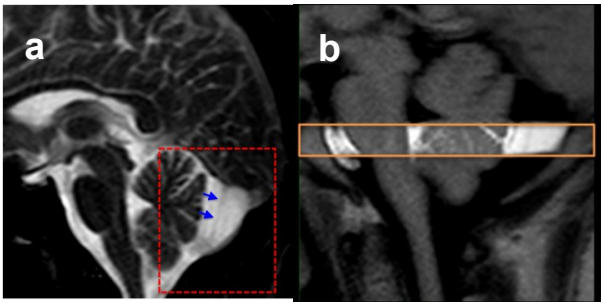

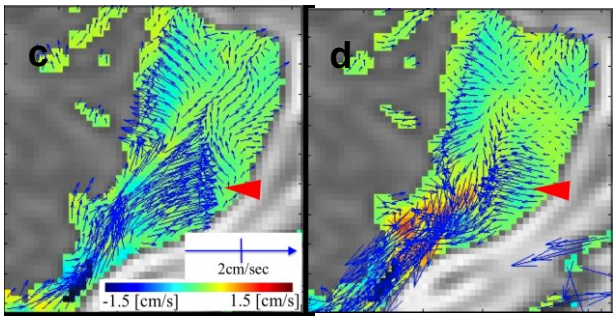

Figure 5. A T2 weighted image (a) of a volunteer with arachnoid cyst, whose membrane-like structure is clearly visualized (blue arrows). Zoomed velocity images of 4D-PC technique around the arachnoid cyst at 9.3% (c) and 81.3% (d) of time periods in a peripheral pulse cycle. The corresponding Time-SLIP image labeled with a slab in the mid portion within the arachnoid cyst (orange rectangle).

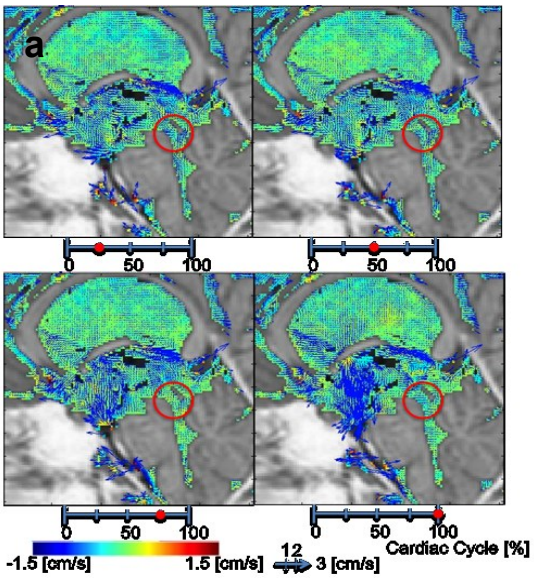

Figure 6. Temporal changes of 4D-velocity within ventricular system of the patient with hydrocephalus. The 4D-PC velocity image showed a slightly lowered velocity amplitude because of membrane in the aqueduct (red circle).

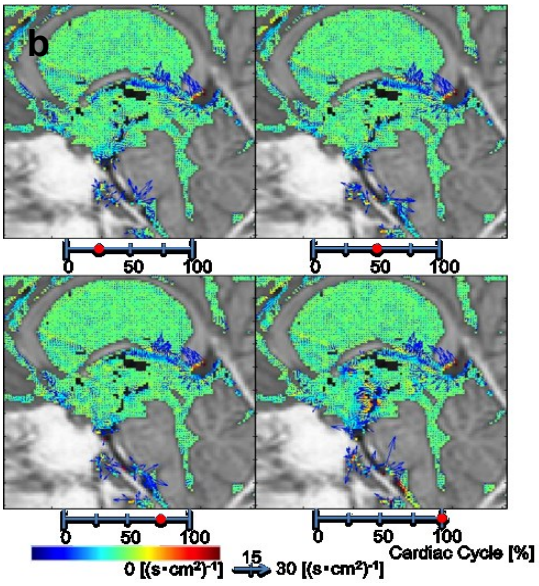

Figure 7. Temporal changes of curl within ventricular system of the patient with hydrocephalus.

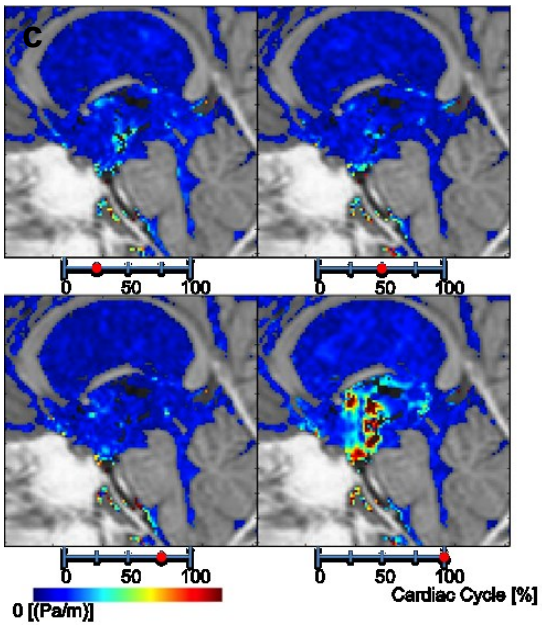

Figure 8. Temporal changes of the pressure gradient within ventricular system of the patient with hydrocephalus.

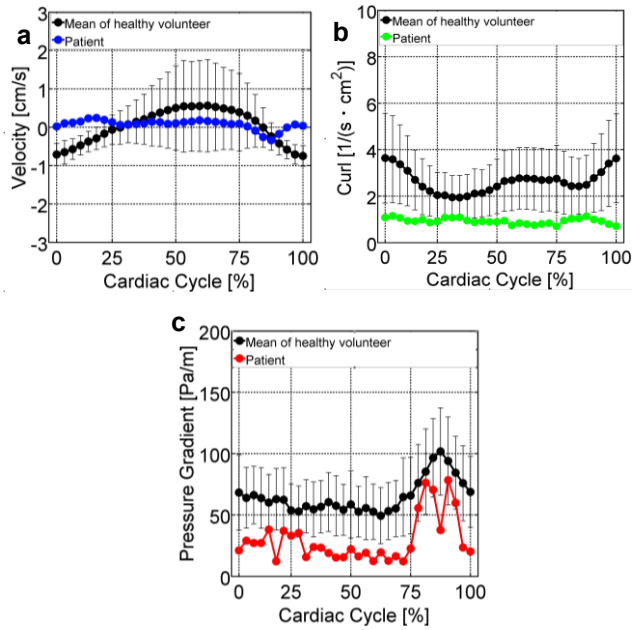

Figure 9. Comparison of the temporal changes of velocity (a), curl (b) and pressure gradient (c) of the patient of obstructive hydrocephalus with the mean velocity, curl and pressure gradient of healthy volunteers. Error bars denote the range of standard deviation of the data.

IV. Discussion

In this study the difference and the usefulness of the 4D-PC techniques in visualizing the CSF flow around the membrane structures were examined in comparison with Time-SLIP technique. In the phantom experiments, the pulsatile fluid separated by a rubber membrane exhibited similar flow pattern in the 4D-PC images because of the pressure propagation. In contrast, fluid labeled in the Time-SLIP technique showed only little displacement due to the small spin traveling distance restricted by the membrane.

The similar phenomen was observed in the volunteer with arachnoid cyst. This result confirmed that the pulsatile CSF flow disrupted by a thin wall structure of the arachnoid cyst may transmitted the pressure gradient to generate the similar velocity waveform to the cephalic or caudal directions beyond the point of the wall. This result suggest that the 4D-PC technique can reveal the propagations of pulsatile CSF motion partitioned by the thin wall of cyst despite that there is no communication between the arachnoid cyst and the neighboring CSF space.

In a patient with hydrocephalus with a membrane-based obstruction at the aqueduct, the propagation of the fluid flow was not clearly visualized. However, when the velocity, curl and pressure gradient were analyzed in the quantitative manner, the flow dynamics was clearly different from that of the healthy volunteer group.

In conclusion, the 4D-PC technique is useful to visualize the CSF dynamics under the presence of a membrane-like structure, unlike the Time-SLIP in which the spin travel is exclusively visualized. Quantitative property is also an advantage of the 4D-PC technique. The curl and the pressure gradient fields are obtained with actual units helping so that clinicians may use the information for classifying the conditions of the patients with CSF disorders.

For further verification of the usefulness of the technique, more patient studies with various CSF disorders are required. We expect this technique to be used for clinical diagnosis of various status of hydrocephalus. Moreover, indication of the driving force and the origin of the CSF pulsation may be possible when this technique is combined with the wave form correlation analyses.

References

[1] Henry-Feugeas MC et al. Magn Reson Imag 2000;18(4):387–95.
[2] Alperin NJ et al. Magn Reson Med 1996;35:741-754.
[3] Naidich TP et al. Neurosurge Clin North Am 1993;4(4):677–705.
[4] Yamada S et al. Radiology 2008:249(2):644–52.
[5] Feynman R, Leighton R, Sands M. The Feynman lectures on physics, Addison Wesley, Longman, 1970.
[6] Chandran K, Rittgers S, Yoganathan A. Biofluid Mechanics: The Human Circulation, Second Edition. Taylor and Francis, Boca Raton, 2012.